Light Metals 2013 *Edited by: Barry Sadler*
TMS (The Minerals, Metals & Materials Society), 2013

Hatch – ETI Aluminyum Precipitation Modeling

E. Stamatiou[1,*], D.R. Chinloy[1], B. Çelikel[2], M. Kayaci[2], E. Savkilioglu[2]
[1]Hatch Ltd., 2800 Speakman Dr, Mississauga, ON, Canada
[2]ETI Aluminyum, Atatürk Caddesi, Seydisehir / KONYA 42370, Turkey
*to whom correspondence should be addressed: astamatiou@hatch.ca

Keywords: Alumina, Hydrate Precipitation Modeling, PSD, Agglomeration, Growth, Nucleation, Attrition.

Abstract

World alumina producers are focusing their efforts on increasing plant efficiency and product quality. The aluminum smelters, the customers of about 90% of the alumina plant product, are requiring a strong and coarse alumina. This demand has lead to more challenging process conditions for the hydrate precipitation process, requiring further fundamental understanding.

This paper describes a methodology to predict the Particle Size Distribution (PSD) of hydrate precipitation using SysCAD steady state process modeling. The process model is validated with data from ETI alumina plant. It is shown that Hatch and ETI Aluminyum have implemented a modified hydrate precipitation circuit that employ a classification system for proper distribution of coarse and fine seed, agglomeration stages, and new particle process control strategies which resulted in hydrate product coarsening from approximately 20%, -44μm to 10%-12%, -44 μm and product yield to over 94 gpl Al_2O_3.

Introduction

Production of alumina by the Bayer process remains, in principle, unchanged since its invention. Although the process has been the subject of large number of technical improvements to decrease energy and manpower, the precipitation area design is based on available empirical correlations, supplemented by operating know how of existing plants. Inadequate knowledge of the fundamental phenomena occurring and of key crystallization variables may lead to the over design of equipment, use of extra equipment or inadequate control schemes to achieve the desired alumina quality specifications. With the low current alumina prices, existing alumina refineries are still in search of ways of producing good quality alumina with low energy. In addition, smelters are converting from Soderberg pots to prebake technology, which requires coarser/stronger hydrate particles. The proper design and operation of the precipitation area is thus critical for optimizing the yield and quality of alumina product.

Over the years, there have been considerable efforts towards the development of hydrate precipitation models to predict both product yield (recovery) and Crystal Size Distribution (CSD) [see Refs. 1 – 11, 13, among others]. These models utilize the population balance in addition to the traditional laws of conservation of mass and energy. Several companies have developed their own proprietary precipitation models, but there has not been a "generic" or "publically" approved population balance model that predicts the alumina PSD in the Bayer precipitation process. Hence our efforts in this paper are focused to present such a generic model for the Bayer engineer.

ETI Aluminyum Hydrate Precipitation Circuit

The original ETI Alumina refinery was designed by VAMI in the late 1960s to produce 200,000 tons per year of semi-floury alumina equivalent with fines (-44 μm) of approximately 25%. Celikel et al. [3] have presented the success on the conversion of ETI's original hydrate precipitation circuit to produce a coarser alumina without impacting the precipitation yield. Figure 1 and Figure 2 give the schematic arrangement for ETI hydrate precipitation circuits before and after the precipitation upgrade. For a detail description of the old and new ETI precipitation circuits the reader is referred to Celikel et al. [3].

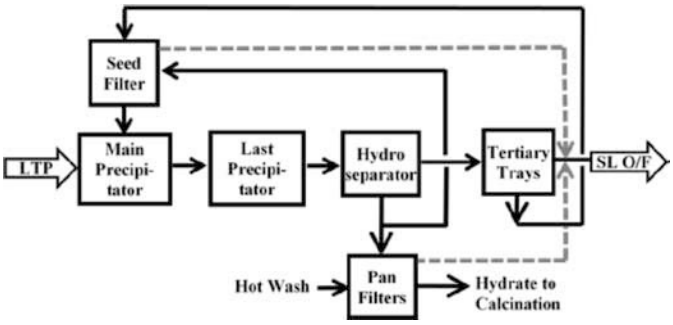

Figure 1. ETI precipitation circuit prior to upgrade.

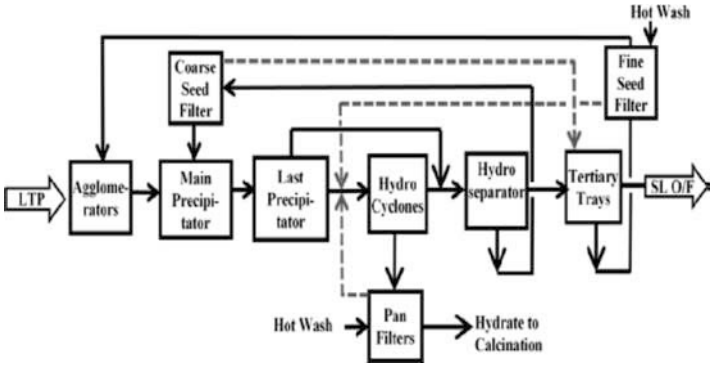

Figure 2. New ETI 2012 precipitation circuit after upgrade.

In comparing the flowsheets of Figure 1 and Figure 2, the main elements of this conversion performed by Hatch and ETI Aluminyum are listed below:

(a) Implementation of an agglomeration section with fine seed matched to the design circuit temperature;
(b) Installation of hydrocyclones clusters to meet product cut size;
(c) Use of product filters for fine seed and coarse seed wash;
(d) Dual charge system with proper distribution of the fine seed and coarse seed to the precipitation circuit;

(e) Installation of steam sparger in the fine seed tank for seed activation;
(f) Practicing of seed activation techniques that include the use of CGM in the agglomeration section.

SEM morphologies of the product hydrate before and after the precipitation conversion are given in Figures 3 and 4, respectively. The SEM photographs from 2012 clearly reveal that the hydrate particles are better cemented together due to the more ideal precipitation conditions promoting stronger hydrate particles.

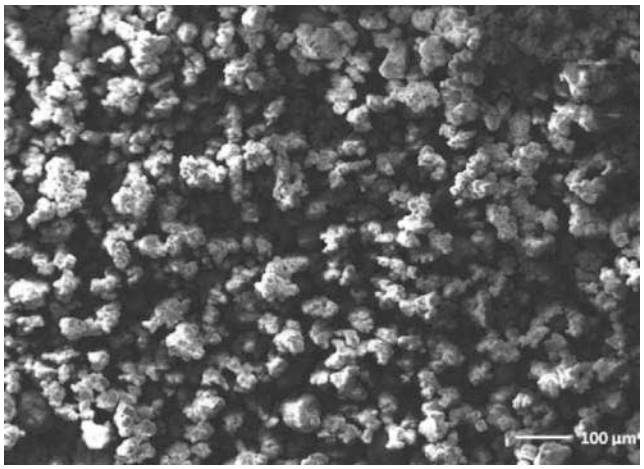

Figure 3. Sample SEM photograph of hydrate prior to conversion.

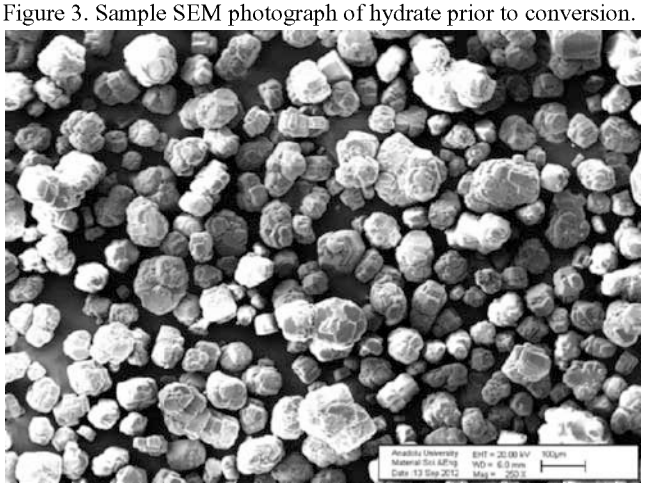
Figure 4. Sample SEM morphology of 2012 ETI hydrate.

In this study, a PSD process model was developed to make predictions of the hydrate PSD and liquor productivity (yield) before and after the modifications of the ETI precipitation circuit. The modeling methodology, results and discussion are presented in the next sections.

The Population Balance Model

A literature review shows that there are three main processes in hydrate precipitation that can alter the crystal size distribution: 1) agglomeration; 2) growth; 3) primary and secondary nucleation and 4) attrition or breakage mechanism. Perry's Chemical Engineers' Handbook [10] provides a useful form of the generalized particle population balance for particulate systems:

$$\frac{\partial n(V,t)}{\partial t} = \frac{Q_{in}}{V} n_{in}(V) - \frac{Q_{out}}{V} n_{out}(V) - \frac{\partial (G-D) n(V,t)}{\partial V} + B(V,t) + Agg(V,t) \quad (1)$$

where V is the control volume of the reactor, n are the number of hydrate particles contained in the control volume, Q_{in} and Q_{out} are the inlet and outlet flow rates out of the control volume, $G(V)$, $D(V)$, $B(V)$, $Agg(V)$ are the growth, death (attrition), birth (nucleation) and agglomeration rates, respectively.

In this paper, a full PSD hydrate precipitation model is presented for ETI Aluminyum plant (Seydisehir, Turkey). The PSD model implements open literature correlations for growth, agglomeration and nucleation mechanisms. The model was successfully implemented using SysCAD v. 9.2 build 134 steady state process simulator with PSD alumina library (see Ref. [12]), which provides the advantage of simulating a full PSD plant model for the entire alumina plant in a graphical and user friendly interface. The paper first describes the model input parameters and conditions required in order to solve Eq. (1), and follows with the results and discussion.

Model Input Parameters

Growth rate

Various well established expressions of the gibbsite growth rate exist in literature (for a list see Farhadi et al. [4], among others):

$$G = K_g \cdot e^{\frac{-\Delta E}{RT}} \cdot \frac{1}{C^{1/g}} \left(\frac{A}{C} - \frac{A_{eq}}{C}\right)^g \quad (2)$$

where G is the linear growth rate, A and A_{eq} are sodium aluminate ion concentrations, K_g and g are constants. The sodium aluminate equilibrium solubility, A_{eq}, was empirically fitted to ETI's plant data. Particle growth increases the total mass of alumina tri-hydrate without changing particle numbers. The constant Kg was determined by curve fitting Eq. (2) to the ETI plant data across the precipitator trains with g = 2 (White and Bateman [13]). The current population balance model assumes spherical particles and does not take into account the geometric correction factor.

Nucleation rate

Hydrate nucleation (both primary and secondary) has been previously studied by Brown [1, 2], Misra and White [9], Halfon and Kaliaguine [5] and Hong et al. [6]. Nucleation deals with the formation of new particles generated in the smallest particle size range (micro or sub-micro). Two types of nucleation have been identified: primary and secondary nucleation. Primary nucleation deals with the creation of new nuclei forming spontaneously from the supersaturated Bayer liquor, while secondary nucleation involves the creation of new nuclei formed at the surface of pre-existing particles. According to Misra and White [9], primary nucleation is a function of supersaturation and temperature, whereas secondary nucleation is a function of solids concentration in the control volume.

The current population balance model uses the nucleation rate expression as originally proposed by Misra and White [9]:

$$B = K_N \cdot SSA \cdot \left(\frac{A - A_{eq}}{C}\right)^2 \quad (3)$$

where A, A_{eq} and C are ion concentrations, K_N is a constant and SSA the specific surface area. The constant in Eq. (3) is determined by best fitting the precipitation data to the ETI

Aluminyum plant data. If the ion concentrations are constant, then the nucleation would be zero.

Agglomeration kernel

The expression $Agg(V,t)$ in equation 1 is the agglomeration kernel and can be defined as a product of the frequency of collisions between particles of volume V and particles of volume V', and the efficiency of agglomeration (i.e. the probability of particles of volume V agglomerating with particles of volume V'). In literature, β is often used to symbolize the agglomeration kernel. Several agglomeration models have been proposed (see Ilievski and White [8] and Ilievski and Livk [7]).

The current population balance model uses the size-dependent agglomeration kernel proposed by Ilievski and White [8]:

$$\beta_{ij} = \frac{G}{\beta_4 S_{ij}} \tag{4}$$

where G is the growth rate, $Sij = L_i + L_j$ are the linear dimensions of the hydrate particle, and β_4 is a constant that was determined by curve fitting the ETI PSD data in the agglomeration section.

Attrition / Breakage

Stephenson and Kapraun [11] proposed that the probability of a fracture of a particle should be proportional to the particle's diameter cubed. In mineral processing, many other attrition mechanisms existing for simulating the breakage of particles and could be readily adopted in the current population balance model with some experimental validation.

In the population balance model, a simple crusher model was implemented at the end of precipitation circuit to simulate the breakage of a selected fraction of particles and their redistribution to smallest mass fractions. The breakdown fraction of the hydrate particles was determined by curve fitting the ETI PSD data in the -44 μm and -20 μm size fraction ranges.

Hydrate Classification

The population balance model also includes modeling of 2007 and 2012 hydrate classification circuits as given in Figures 1 and 2, respectively. This section describes the modeling details of the hydrate classification system.

The efficiency values in the hydrocyclones model were selected based on cyclone performance PSD and mass balance data provided by the equipment vendor. Hydroseparators, trays as tertiaries, fine seed and coarse seed and hydrate filters are full PSD screen-type models that were empirically fitted to the ETI plant data.

Results and Discussion

Table I summarizes the 2007 and 2012 main precipitation circuit parameters (average) that were used to construct the PSD hydrate model.

Table I. PSD Plant Data for 2007 and 2012 ETI circuits

Description	Units	2007	2012
Agglomerators in Service	#	-	2
Growth Tanks in Service	#	17	15

The model calibration kinetic parameters for growth, agglomeration and nucleation (Kg, K_{agg} and K_N) were fitted to the plant data; the tuning parameters were kept identical in the 2007 and 2012 precipitation circuits. The breakdown function was calibrated to match the -44 μm fraction in the PSDs from 2007 and 2012 circuit, respectively. It was determined that the breakdown function was significantly larger in the 2007 precipitation circuit. As a result of the precipitation circuit improvements described above, the percentage of the particles breaking down to smaller fractions was reduced in 2012.

Table II compares the plant data with the PSD model distributions, final A/C ratios and liquor productivity (yield) for both 2007 and 2012 precipitation circuits. The liquor productivity was calculated according to the definition given by Celikel et al. [3]

$$Yield\left(\frac{g}{L}Al_2O_3\right) = \left[\frac{0.962}{\alpha_{k,in}} - \frac{0.962}{\alpha_{k,out}}\right] \cdot C_{in} \tag{5}$$

where $\alpha_{k,in}$ and $\alpha_{k,out}$ are the caustic modulus at the inlet and outlet of the precipitation circuit, and C_{in} is the caustic concentration at the inlet of precipitation in gpl Na_2CO_3. As shown in Table II below, the simulation results match very well the plant data.

Table II. PSD Plant and Model Results for 2007 and 2012 Hydrate Precipitation Circuits

Year		2007	2012
Plant Data			
Liquor productivity	gpl	83.8	94.0
-44 μm hydrate fraction	%	19.6	9.3
D50	μm	70	78
Model Last Precipitator PSD			
149 μm	%Passing	90.6	98.9
74 μm	%Passing	53.8	58.2
44 μm	%Passing	24.7	14.4
20 μm	%Passing	6.1	2.0
Model Hydrate Filter PSD			
149 μm	%Passing	90.1	96.4
74 μm	%Passing	51.6	39.6
44 μm	%Passing	21.5	7.0
D50	μm	72.3	69.0
Model Overall			
Production	tph as Al_2O_3	22.0	28.2
Caustic	as Na_2CO_3	243.2	228.4
A/C out	-	0.277	0.268
Yield Calculated	gpl Al_2O_3	83.0	93.0

Figure 5 compares the PSD model distributions with plant PSD data in a graphical format. In comparing the cumulative distribution data in Figure 5, one can readily see that the 2007

PSD data in the lower particle classes (less than 44 microns) shift to larger fraction classes in 2012.

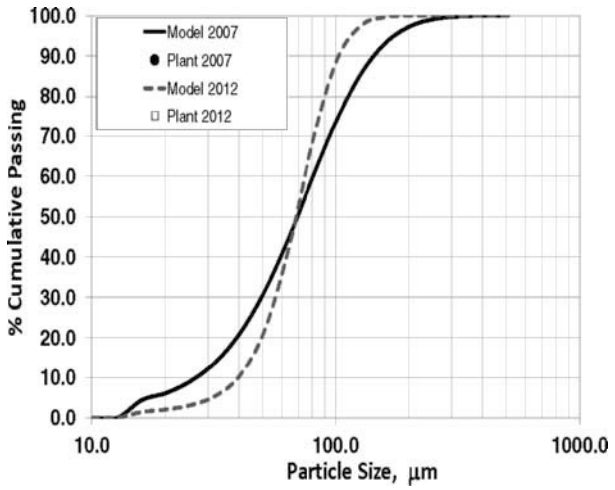

Figure 5. Cumulative model PSDs compared to ETI plant data for last decomposer.

Figure 6 compares the D50 simulation values across the precipitation train with plant data from 2007 and 2012, respectively. The results indicate that the precipitation conditions implemented in 2012 promoted stronger hydrates particles as also indicated by the reduction in the -44 µm fraction (change from more than 20% in 2007 to less than 10% in 2012).

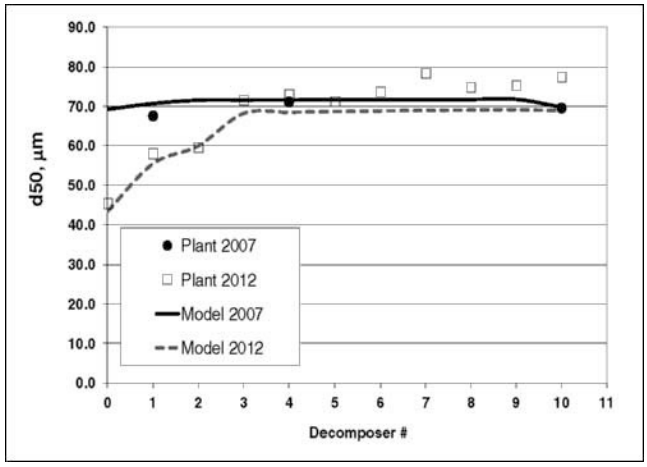

Figure 6. D50 simulation values along precipitation train compared to plant data from 2007 and 2012, respectively.

The current PSD precipitation model presented in this study curved fitted to ETI plant indicates that the hydrate product in 2007 was weaker and that the 2012 hydrate particles have less breakage.

Conclusions

In this work, a full PSD hydrate process model was presented fitted to the 2007 and 2012 precipitation circuits, which supported an improvement in the hydrate quality and strength that was achieved by implementing the modified hydrate precipitation circuit.

Implementing a full PSD process model that captures the correct physics of hydrate particles including growth, agglomeration, nucleation and attrition mechanisms will allow a tighter control of hydrate product quality as well as monitoring of the fines population balance in the precipitation circuit, information which cannot be captured by a simple mass balance alone.

The modified precipitation process implemented at ETI alumina refinery increased the liquor productivity by about 10-12% from 84 gpl to 94 gpl Al_2O_3 while at the same time reducing the -44 µm fraction of fines from approximately 20 to about 10%. The hydrate particles are stronger.

Acknowledgements

The authors wish to acknowledge ETI Aluminyum for their support of these R&D studies, and thank ETI Aluminyum and Hatch for permission to publish this paper.

References

1. N. Brown, "Secondary nucleation of aluminum trihydroxide," *J. Crystal Growth*, 16 (1972), 163-167.
2. N. Brown, "Secondary nucleation of aluminum trihydroxide kinetics and mechanism," *Light Metals* (1976), 1-14.
3. B. Celikel, G.K. Demir, M. Kayaci, M. Baygul, C.E. Suarez, "Precipitation area upgrade at ETI Aluminum," *Light Metals*, (2012), 129 – 133.
4. F. Farhadi, M.B. Babaheidary, "Mechanism and estimation of Al(OH)3 crystal growth, " *J Crystal Growth*, 234 (2002), 721-730.
5. A. Halfon, S. Kaliaguine, "Alumina Trihydrate crystallization. Part 1, secondary nucleation and growth kinetics," *Can J. Chem Eng*, 54 (1976), 160.
6. X. Hong X, B. Shiwen B., S. Shiwu, C. Wankun, Y. Yinhong, L. Dianfong, "Secondary nucleation of aluminum tihydroxide in bayer sodium aluminate solution," *Light Metals* (1995), 101-104
7. D. Ilievski and I. Livk, "An agglomeration efficiency model for gibbsite precipitation in turbulently stirred vessel," *Chem Eng. Sci.*, 61 (2006), 2010- 2022.
8. D. Ilievski and E.T. White, "Modeling Bayer precipitation with Agglomeration," *Light Metals* (1995), 55 - 61.
9. C. Misra and E.T. White, "Kinetics of crystallization of alumina trihydroxide from seeded caustic alumina solutions," *Chem. Eng. Progress Symp. Ser*, 67 (110) (1971), 53-65.
10. R.H. Perry and D.W. Green, *Perry's Chemical Engineers' Handbook*, (New York: McGraw-Hill, 1997), 7th edition, 20.85.
11. J.L. Stephenson and C. Kapraun, "Dynamic modeling of yield and particle size distribution in continuous Bayer precipitation," *Light Metals* (1997), 89 – 95.
12. SysCAD User's Manual 2012, "Alumina3 Precip – Full PSD," http://help.syscad.net/index.php/Alumina3_Precip_-_Full_PSD, accessed on Oct 23, 2012.
13. E.T. White and S.H. Bateman, "Effect of Concentration on the Growth Rate of Al(OH)3 Particles," *Light Metals* (1998), 157–162.